Carcinogenesis vol.29 no.10 pp.2035–2043, 2008
doi:10.1093/carcin/bgn188
Advance Access publication August 9, 2008

RAGE, carboxylated glycans and S100A8/A9 play essential roles in colitis-associated carcinogenesis

Olga Turovskaya, Dirk Foell[1], Pratima Sinha[2], Thomas Vogl[3], Robbin Newlin[4], Jonamani Nayak[4], Mien Nguyen[4], Anna Olsson[4,7], Peter P.Nawroth[5], Angelika Bierhaus[5], Nissi Varki[6], Mitchell Kronenberg, Hudson H.Freeze[4] and Geetha Srikrishna[4,*]

Division of Developmental Immunology, La Jolla Institute for Allergy and Immunology, La Jolla, CA, USA, [1]Department of Pediatrics, University of Münster, Münster, Germany, [2]Department of Biological Sciences, University of Maryland, Baltimore County, Baltimore, MD, USA, [3]Institute of Experimental Dermatology, University of Münster, Münster, Germany, [4]Tumor Microenvironment Program, Cancer Center, The Burnham Institute for Medical Research, La Jolla, CA, USA, [5]Department of Medicine, University of Heidelberg, Heidelberg, Germany and [6]Department of Pathology, University of California at San Diego, La Jolla, CA, USA

[7]Present address: Clinical Trials, Capio Diagnostik, Nygaardsvej 32, DK-2100 Copenhagen, Denmark

[*]To whom correspondence should be addressed. Tel: +1 858 795 5256; Fax: +1 858 713 6281;
Email: gsrikrishna@burnham.org

Patients with inflammatory bowel diseases are at increased risk for colorectal cancer, but the molecular mechanisms linking inflammation and cancer are not well defined. We earlier showed that carboxylated N-glycans expressed on receptor for advanced glycation end products (RAGE) and other glycoproteins mediate colitis through activation of nuclear factor kappa B (NF-κB). Because NF-κB signaling plays a critical role in the molecular pathogenesis of colitis-associated cancer (CAC), we reasoned that carboxylated glycans, RAGE and its ligands might promote CAC. Carboxylated glycans are expressed on a subpopulation of RAGE on colon cancer cells and mediate S100A8/A9 binding to RAGE. Colon tumor cells express binding sites for S100A8/A9 and binding leads to activation of NF-κB and tumor cell proliferation. Binding, downstream signaling and tumor cell proliferation are blocked by mAbGB3.1, an anti-carboxylate glycan antibody, and by anti-RAGE. In human colon tumor tissues and in a mouse model of CAC, we found that myeloid progenitors expressing S100A8 and S100A9 infiltrate regions of dysplasia and adenoma. mAbGB3.1 administration markedly reduces chronic inflammation and tumorigenesis in the mouse model of CAC and RAGE-deficient mice are resistant to the onset of CAC. These findings show that RAGE, carboxylated glycans and S100A8/A9 play essential roles in tumor–stromal interactions, leading to inflammation-associated colon carcinogenesis.

Introduction

Colorectal cancer remains one of the most diagnosed and leading causes of cancer-related deaths worldwide. Patients with inflammatory bowel disease are at a higher risk for developing colorectal cancer than the general population. Several lines of evidence point to chronic inflammation of the colon as an important factor in the progression to colorectal cancer in inflammatory bowel disease (reviewed in ref. 1). However, the molecular basis of the association between inflammation and cancer remains poorly understood. Prolonged proinflammatory signaling and defective anti-inflammatory responses lead to a state of persistent inflammation. Inflammatory cells, particularly macrophages, produce soluble factors including cytokines, growth and angiogenic factors and matrix metalloproteinases, creating a microenvironment that supports proliferation, invasion and metastasis of transformed cells (2,3). Specific inactivation of the classical nuclear factor kappa B (NF-κB) activation pathway in colonic epithelial cells and macrophages reduces the formation of inflammation-associated colonic tumors in mice, suggesting that sustained NF-κB activation in either or both of these cells may provide a critical link between inflammation and cancer (4,5). Identifying molecular interactions leading to activation of NF-κB in colon tumors could therefore provide further understanding of tumor–stromal cell cross talk and the mechanisms underlying inflammation-based colon carcinogenesis.

The receptor for advanced glycation end products (RAGE) is a multiligand signaling receptor of the immunoglobulin superfamily implicated in inflammation and cancer among other pathologies (6–8). RAGE interaction with proinflammatory mediators such as S100 proteins and high-mobility group box 1 (HMGB1) leads to intracellular activation of NF-κB. RAGE promoter has NF-κB-binding sites (9), and pathological accumulation of RAGE ligands enhances expression of the receptor thus ensuing a cycle of sustained NF-κB activation and prolonged cellular response (10). RAGE binds multiple structurally diverse ligands and is considered a pattern recognition receptor, but the structural basis for RAGE binding to multiple ligands is not well understood. We identified a group of anionic N-glycans that contain an immunogenic carboxylate group unrelated to sialic or uronic acids (11,12). These carboxylated glycans appear to contain glutamic or aspartic acids probably linked to glucosamine of the sugar chain (13). In normal tissues, carboxylated glycans show restricted expression on cells of myeloid lineage, especially macrophages and dendritic cells, and on endothelial cells and are recognized by HMGB1, S100A8/S100A9, S100A12 and annexin-1 (11,14,15). RAGE is modified by carboxylated glycans and the glycans mediate binding of HMGB1 and S100A12 to RAGE (14) and (G.Srikrishna and H.H.Freeze, unpublished results). In a mouse model of T cell-mediated colitis, we found upregulation of expression of RAGE and carboxylated glycan-binding lectins S100A8/A9 in secondary lymphoid organs and in colonic lamina propria early in inflammation. In this model, mAbGB3.1, an anti-carboxylated glycan antibody, blocked onset of colitis and reversed colitis in the early stage of disease by blocking NF-κB signaling (16).

S100A8/A9 proteins, members of the EF-hand calcium-binding proteins secreted by neutrophils and activated monocytes (17), function as heterodimers and induce activation of NF-κB (18–20). They are elevated in numerous conditions associated with inflammation, such as rheumatoid arthritis, cystic fibrosis and in inflammatory bowel disease (reviewed in refs 21–23). In addition, strong upregulation of these proteins has also been found in many tumors (reviewed in ref. 21). Elevated expression of S100A8/A9 both in inflammation and in cancer suggests that they may play important roles in inflammation-induced cancers. RAGE and S100A8/A9 are coexpressed in tumors (18,24,25) and are linked to downstream signaling in tumor cells and

Abbreviations: AOM, azoxymethane; BSA, bovine serum albumin; CAC, colitis-associated cancer; DSS, dextran sulfate sodium; HBSS, Hanks' balanced salt solution; HMGB1, high-mobility group box 1; IL, interleukin; MDSC, myeloid-derived suppressor cell; NF-κB, nuclear factor kappa B; PBS, phosphate-buffered saline; PNGase F, peptide N-glycanase F; RAGE, receptor for advanced glycation end products; TLR4, Toll-like receptor 4; TNFα, tumor necrosis factor alpha.

endothelial cells (18,25,26). RAGE binds many S100 proteins, but whether it directly binds S100A8/A9 remains unanswered. More recent studies provide evidence that such interactions are likely (25,27).

In the present study, we tested the hypothesis that carboxylated glycans, RAGE and carboxylated glycan-binding proteins S100A8/A9 exert tumorigenic functions in the setting of inflammation. A recent report, published when this manuscript was in preparation, illustrates the importance of RAGE signaling in inflammation-mediated skin carcinogenesis (28). We extend these findings and show that RAGE signaling also promotes the development of colitis-associated cancer (CAC). In addition, we demonstrate that carboxylated glycans mediate S100A8/A9 and RAGE binding and that these glycans promote receptor-mediated signaling, leading to the pathogenesis of CAC.

Materials and methods

Human tissues

Paired tumor and normal adjacent colon tissue samples ($n = 9$) snap frozen in liquid nitrogen after surgery were provided by the Cooperative Human Tissue Network (National Cancer Institute). Samples were from both male and female patients in the age range from 52 to 80 years. Pathology reports were provided by Cooperative Human Tissue Network for each tissue sample and included well-differentiated, moderately differentiated and poorly differentiated adenocarcinomas (American Joint Committee on Cancer staging: two cases of stage I, one case of stage IIA, one case of stage IIB, one case of stage IIIB, three cases of stage IIIC and one case of stage IV). Five micrometer cryosections were made and stored frozen until analysis.

Mice

$RAGE^{-/-}$ mice were generated as described (29). They were backcrossed to C57BL/6 mice for >10 generations. Six- to 8-week-old $RAGE^{-/-}$ mice, $RAGE^{+/+}$ littermates or age-matched wild-type mice were used for experiments. All animal protocols were approved by the Burnham Institute for Medical Research Institutional Animal Care and Use Committee and were in compliance with National Institutes of Health policies.

Tumor induction

CAC was induced in mice using azoxymethane (AOM) and single cycle of dextran sulfate sodium (DSS) as described (30). Animals were constantly monitored for clinical signs of illness and were sacrificed at the end of 2, 6, 12 or 20 weeks after DSS. Blood samples were collected by retro-orbital bleeding prior to induction of disease and at time points as above. In the preventive protocol of antibody treatment, mAbGB3.1 (10 μg/g) was administered intravenously in 100 μl phosphate-buffered saline (PBS) once a week, until 6 or 12 weeks of disease initiation. For every time point, separate groups of control mice were either left untreated or administered an equivalent amount of a non-specific isotype control antibody. In the therapeutic protocol, mice received the antibodies weekly starting 6 weeks after initiation of disease and killed at 12 weeks. Separate groups of $RAGE^{-/-}$ mice or age-matched control mice were subjected to the same AOM–DSS protocol and sacrificed at 2, 6 or 20 weeks after disease initiation. At each time point, colons were excised, fixed as 'Swiss-rolls' in 4% buffered formalin and embedded in paraffin or fixed in optimal cutting temperature. Stepwise sections were cut and stained with hematoxylin and eosin. Colonic inflammation, dysplasia and neoplasms were graded based on described criteria (30) by a pathologist blinded to the conditions. Immunochemical analysis was done as described below.

Immunochemical analysis

Immunochemical analysis of frozen human tissue sections was done as described earlier (11) except for the following modifications: before fixing in formalin, sections were immersed in 0.03% H_2O_2 for 30 min at room temperature, blocked with 1% bovine serum albumin (BSA)/PBS for 20 min followed by 0.1% avidin and 0.01% biotin in succession for 15 min at room temperature in a humid chamber with PBS washes in between. The following antibodies were used for staining: mAbGB3.1, anti-human RAGE (11F2, kind gift of Novartis Foundation, Tokyo, Japan) or anti-human S100A9 (Novus Biologicals, Littleton, CO). After counterstaining, the slides were scanned into Aperio Imaging system and were also observed under a bright-field microscope and images acquired as given below.

Fixed mouse colon sections (6 μm) were deparafinized and rehydrated in PBS; endogenous peroxidases were neutralized with 1% hydrogen peroxide and blocked with avidin/biotin (Vector Laboratories, Burlingame, CA). Samples were then incubated with anti-mouse S100A8 or anti-mouse S100A9 (goat polyclonal, R&D Systems, Minneapolis, MN), followed by biotin-conjugated secondary antibody. Binding was detected using streptavidin–peroxidase complex (Vector Laboratories) and diaminobenzidine (DAKO, Carpinteria, CA). Sections were then counterstained with hematoxylin. To characterize leukocyte populations, sections were stained with anti-mouse CD11b, anti-mouse Gr-1 (BDPharmingen, San Diego, CA) or both followed by Alexa 594 or Alexa 488-conjugated secondary antibodies (Invitrogen, Carlsbad, CA) and cover slipped with VectaShield DAPI Mounting Medium (Vector Laboratories). Slides were examined using an Inverted TE300 Nikon Wide Field and Fluorescence Microscope and images were acquired with a CCD SPOT RT Camera (Diagnostic Instruments, Sterling Heights, MI) using SPOT advanced software.

Cells

HT-29, Caco-2 and CT-26 tumor cell lines were obtained from American Type Culture Collection (Manassas, VA) and maintained in Dulbecco's modified Eagle's medium containing glutamine, penicillin and streptomycin and 10% fetal bovine serum. Cells were harvested using PBS with 5 mM ethylenediaminetetraacetic acid. Cell membranes were generated by homogenization in PBS with protease inhibitors (Roche Diagnostics, Indianapolis, IN). Nuclei and cell debris were removed by centrifugation at 300*g* for 10 min at 4°C. Resulting supernatants were ultracentrifuged at 110 000*g* for 30 min at 4°C, pellets were resuspended in 200 μl of PBS, protease inhibitors and 1% Nonidet P-40 and membrane proteins were extracted by slow stirring overnight at 4°C. Proteins were subjected to deglycosylation using peptide N-glycanase F (PNGase F). For mAbGB3.1 immunoprecipitation, membrane proteins were incubated with mAbGB3.1-coupled Affigel beads in PBS. After overnight incubation at 4°C, the individual pellets were washed to remove unbound label, and bound proteins were eluted with 0.2% sodium dodecyl sulfate/1% 2-mercaptoethanol.

Purification of bovine RAGE and mAbGB3.1 enrichment

Fresh frozen bovine lung was homogenized in 20 mM Tris–HCl, pH 7.4, containing protease inhibitors, 10 mM dithiothreitol, 1 mM $CaCl_2$ and 1% Nonidet P-40. The suspension was centrifuged at 650*g* for 15 min and then at 10 000*g* for 30 min and the supernatant was enriched for RAGE using sequential ammonium sulfate precipitation (33% followed by 50%). Precipitate obtained from 50% ammonium sulfate was collected by centrifugation at 10 000*g* for 30 min, dissolved in PBS with 1% Nonidet P-40 and dialyzed extensively against the same buffer to remove ammonium sulfate. RAGE was further purified by first preclearing over rat IgG-immobilized Protein G Sepharose followed by affinity purification over rat monoclonal anti-RAGE (11F2)-immobilized Protein G Sepharose. Bound RAGE was eluted with 0.1 M triethanolamine, pH 11.5, and neutralized using 1 M Tris–HCl, pH 7.5. Contaminant bovine IgG was removed by passing through Protein G Sepharose. Homogeneity was assessed on sodium dodecyl sulfate–polyacrylamide gel electrophoresis gels as described below. For mAbGB3.1 enrichment, the purified protein was incubated with mAbGB3.1-immobilized Affigel-10 beads twice, and bound protein was released using base as above.

Electrophoresis and western blots

Twenty micrograms of membrane proteins from tumor cells before and after deglycosylation or membrane proteins immunoprecipitated by mAbGB3.1 from 1 mg starting material were electrophoresed on denaturing and reducing 12% polyacrylamide gels and transferred to nitrocellulose membranes. The blots were blocked with 10% dry skimmed milk, washed and incubated with a rabbit polyclonal anti-RAGE followed by alkaline phosphatase-conjugated secondary antibody. Staining was visualized using BCIP/NBT (Sigma, St Louis, MO). One microgram purified RAGE or 5 μg purified S100A8/A9 was analyzed on 12 or 17% sodium dodecyl sulfate–polyacrylamide gel electrophoresis gels, respectively, and stained by Coomassie brilliant blue. Purified RAGE was examined by western blot using anti-RAGE before and after EndoH and PNGase F deglycosylation and before and after mAbGB3.1 immunoprecipitation.

Ligand binding assay

S100A8/A9 proteins were purified as described earlier (31) and purity assessed by gels. The complex was added at increasing concentrations to the wells of a 96-well enzyme-linked immunosorbent assay plate containing immobilized total bovine RAGE, RAGE deglycosylated under non-denaturing conditions using PNGase F or mAbGB3.1-enriched RAGE. Incubations were done in Hanks' balanced salt solution (HBSS) containing 1 mM $CaCl_2$ and 1% BSA overnight at 4°C. Bound S100A8/A9 was quantified using goat anti-S100A8, followed by anti-rabbit IgG alkaline phosphatase conjugate and *p*-nitrophenyl phosphate substrate, against standard S100A8/A9. RAGE bound to the plates was quantified independently using anti-RAGE. Non-specific binding was determined by incubation of S100A8/A9 in wells blocked with BSA alone or in wells coated with mock immunoprecipitates of mAbGB3.1

and blocked with BSA. Non-linear regression analysis was done using GraphPad Prism.

For radiolabeled protein-binding assay, purified mouse S100A8/A9 heterodimeric complex was labeled with $Na^{125}I$ using Iodobeads (Pierce, Rockford, IL), as per the manufacturer's protocol. CT-26 colon carcinoma cells were harvested using PBS containing 10 mM ethylenediaminetetraacetic acid and were stripped of surface-bound endogenous S100A8/A9 by brief incubation in 50 mM glycine and 100 mM NaCl, pH 3.0, for 3 min at 4°C followed by neutralization with cold HBSS. Cells were incubated with increasing concentrations of radiolabeled S100A8/A9 for 1 h at 4°C in HBSS. They were then washed twice with 1 ml of HBSS, solubilized in 0.2 ml of 0.5 M NaOH and cell-bound radioactivity was counted. Non-specific binding was determined by binding in the presence of 50-fold molar excess of cold ligand. Where indicated, binding was carried out in the presence of 10-fold molar excess of mAbGB3.1, isotype control antibody, anti-RAGE or anti-S100A8. Saturation binding kinetic analyses were performed using GraphPad Prism. Values were normalized for number of cells.

NF-κB reporter assay

CT-26 cells were cultured overnight in 24-well plates (2×10^5 cells per well). Cells were transiently transfected with 1 μg of plasmid DNA comprising 0.1 μg of pNF-κB-Luc, containing a luciferase complementary DNA under a regular TATA box and an enhancer element with five NF-κB-binding sites (Stratagene, La Jolla, CA), 0.1 μg of pRL-TK construct [containing *Renilla reniformis* luciferase gene under the thymidine kinase promoter (Promega, Madison, WI)] and inert filler plasmid, using Lipofectamine 2000 (Invitrogen) according to the manufacturer's instructions. Six hours after transfection, cells were placed in low-serum medium for 18 h and stimulated with endotoxin-free S100A8/A9 (0.5 μg/ml, ∼20 nM) in the presence or absence of inhibitors. Twenty-four hours after activation, cells were harvested and enzymes were measured in lysates. The luciferase activities were determined using the Dual-Luciferase Reporter Assay System (Promega) according to the manufacturer's protocol. Transfected unactivated cells accounted for endogenous activity.

Cell proliferation assay

CT-26 cells were plated in 96-well culture plates in 100 μl of 1% serum medium and grown with and without mouse S100A8/A9 in the presence or absence of mAbGB3.1, anti-RAGE or control antibody. Proliferation was measured using 3-(4,5-dimethylthiazol-2-yl)-5-(3-carboxymethoxyphenyl)-2-(4-sulfophenyl)-2H-tetrazolium) (MTS) assay (CellTiter96 Aqueous One Cell Proliferation, Promega) as per the manufacturer's instructions.

Serum cytokines

Serum tumor necrosis factor alpha (TNFα) and interleukin (IL)-6 were measured using ELISA Kits (Biosource, Invitrogen, Carlsbad, CA) as per the manufacturer's protocol.

Statistical analysis

Statistical comparisons were performed using one-way analysis of variance or Student's *t*-test. Differences were considered statistically significant when $P < 0.05$.

Results and discussion

Expression of carboxylated glycans, RAGE and S100A8/A9 in colorectal tumors

We earlier showed that carboxylated glycans are expressed on endothelial cells and macrophages in normal human colon and on inflammatory infiltrates in colon tissues from patients with colitis (16). To determine whether carboxylated glycans, RAGE and S100A8/A9 are also expressed in colon tumors, we performed immunohistochemistry of human colorectal tumor tissues. Carboxylated glycans, as seen by staining with mAbGB3.1, and RAGE were expressed on endothelial cells and macrophages in almost all the colon tumor tissues and paired adjacent normal tissues (Figure 1). Staining of tumor vasculature by mAbGB3.1 was more intense in a few tumor samples. In addition, in one moderately differentiated colon carcinoma (stage IIIB) there was staining of tumor epithelial cells by both mAbGB3.1 and anti-RAGE, whereas adjacent normal epithelial cells were negative. Few S100A9-positive macrophages were present in normal colon. However, positive cells were found within tumor stroma in all tumor tissues examined (Figure 1). Cells were also positive for S100A8 (data not shown). Increased expression of RAGE on colon tumor epithelial cells and of S100A8/A9 in tumor stroma has also been reported earlier (32–34).

To examine whether RAGE expressed on tumor cells is modified by carboxylated glycans, we analyzed membrane preparations from cultured colon tumor cells. RAGE is expressed on mouse and human colon tumor cells and is glycosylated as evident from a band shift upon PNGase F deglycosylation (Figure 2A). Cell surface

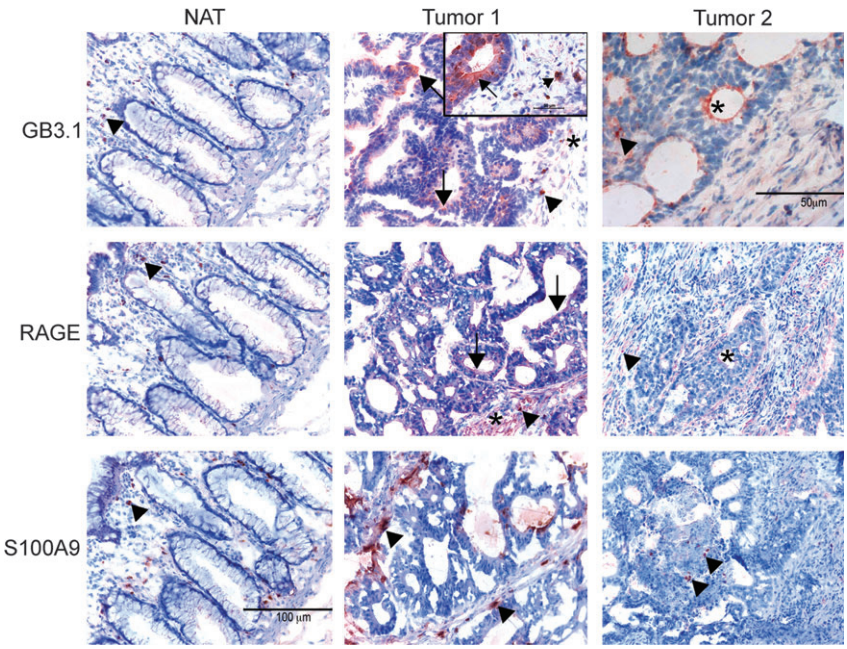

Fig. 1. Expression of mAbGB3.1 glycans, RAGE and S100A9 in human colorectal tumors. Representative immunostained tumor sections and paired normal adjacent tissue (NAT) for tumor 1 are shown. (tumor 1, stage IIIB; tumor 2, stage IIIC; arrowhead, macrophages; asterisk, endothelial cells; arrow, tumor cells). Tumor cells are characterized by hyperchromatic nuclei (intense hematoxylin staining). Bar = 100 μm for all images except for mAbGB3.1 staining of tumor 2 that is enlarged to show staining of tumor vasculature and for the inset for tumor 1 to show distinct mAbGB3.1 staining of tumor cells and macrophages (bar = 50 μm).

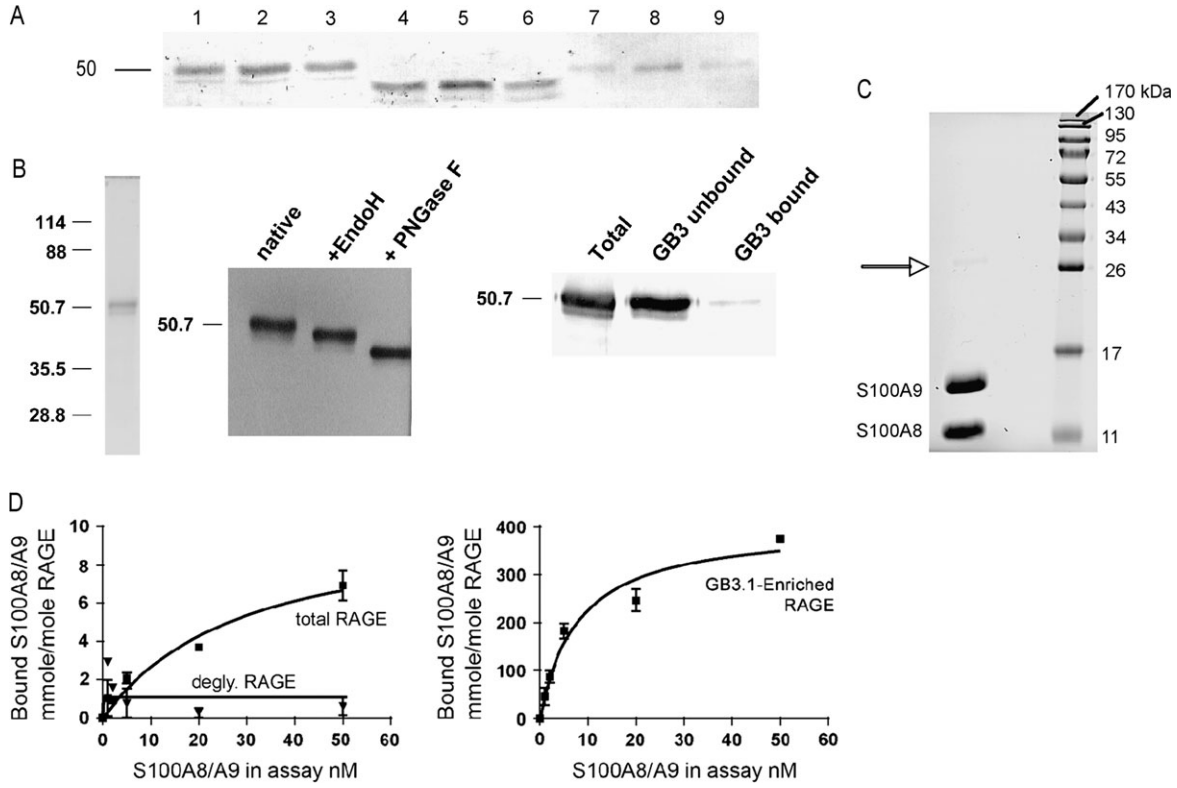

Fig. 2. (**A**) Colon tumor cells express RAGE and mAbGB3.1 glycans. Cell membrane proteins from CT-26 cells (lanes 1, 4 and 7), HT-29 cells (lanes 2, 5 and 8) and Caco-2 cells (lanes 3, 6 and 9) were examined for RAGE expression by western blot using anti-RAGE before deglycosylation (lanes 1–3, 20 μg protein per lane) and after deglycosylation (lanes 4–6, 20 μg protein per lane) and after mAbGB3.1 immunoprecipitation (lanes 7–9, immunoprecipitated from 1 mg of membrane proteins). (**B**) Purification of bovine lung RAGE and mAbGB3.1 enrichment. Left panel: protein stain by Coomassie brilliant blue of a representative RAGE preparation from bovine lung shows >98% purity. Middle panel: western blot using anti-RAGE shows that purified RAGE carries EndoH-sensitive and PNGase F-sensitive N-glycan chains. Right panel: western blot using anti-RAGE shows that mAbGB3.1 immunoprecipitates a minor subpopulation of RAGE. (**C**) Purified mouse S100A8/A9. S100A8/A9 complex was purified as described before, and 5 μg protein analyzed on 17% gels and purity confirmed by Coomassie brilliant blue. Arrow marks the position of covalently linked 26 kDa dimer of S100A8/A9. (**D**) S100A8/A9 complex binds purified RAGE. To determine saturation kinetics of binding of mouse S100A8/A9 to purified RAGE, increasing amounts of S100A8/A9 were added to total RAGE, mAbGB3.1-enriched RAGE or RAGE deglycosylated using PNGase F under non-denaturing conditions that removed both N-glycans. RAGE on plate was quantified using anti-RAGE. Bound S100A8/A9 was quantified using anti-S100A8 against standard S100A8/A9. Data were fitted to non-linear regression analysis using GraphPad Prism. Each point is the mean ± SD of two determinations.

expression of RAGE and carboxylated glycans on tumor cells was confirmed by flow cytometry (data not shown). Less than 2% of RAGE from colon tumor cells was immunoprecipitated by mAbGB3.1, suggesting that RAGE from tumor cells could be modified by carboxylated glycans (Figure 2A). Since yields of RAGE from tumor cells were low, to further confirm whether only a subpopulation of RAGE molecules is modified by carboxylated glycans, we purified RAGE to >98% homogeneity from bovine lung, a rich source of the protein. Homogeneity was confirmed by Coomassie and silver staining (Figure 2B). Treatment with EndoH and PNGase F showed that both N-glycosylation sites on RAGE were occupied by EndoH-sensitive glycan chains and by EndoH-resistant, PNGase F-sensitive chains (Figure 2B). When purified RAGE was incubated with mAbGB3.1, a majority of RAGE remained unbound, even after two rounds of incubation with mAbGB3.1-immobilized beads. Only 5% of total RAGE bound to mAbGB3.1 and could be eluted by high pH or by carboxylated glycopeptides (Figure 2B). This enriched fraction of RAGE showed >10-fold increase in mAbGB3.1 reactivity compared with total RAGE. Most of the binding was lost upon deglycosylation, suggesting that it was glycan dependent (supplementary Figure 1 is available at *Carcinogenesis* Online). We also expressed soluble human RAGE in HeLa cells and found that 1–2% of RAGE express carboxylated glycans (data not shown). These findings confirmed that carboxylated glycans are expressed on a subpopulation of RAGE molecules.

S100A8/A9 complex binds to a subpopulation of RAGE expressing carboxylated glycans

RAGE binds many S100 family proteins including S100A12, S100A1, S100B and S100P and the interactions lead to intracellular signaling (35–37). However, direct binding of S100A8/A9 to RAGE has not been demonstrated. We found that S100A8/A9 complex binds to carboxylated N-glycans (15). Recent studies have used coimmunoprecipitation, RAGE knockdown and protease protection assays to provide more direct evidence for interaction of S100A8/A9 to RAGE (25,27). These studies suggest that S100A8/A9 may directly bind to RAGE on the cell surface or that RAGE may be an integral part of an S100A8/A9 binding complex. To determine if S100A8/A9 directly bound RAGE and to examine the role of carboxylated glycans in binding, we incubated increasing amounts of purified mouse S100A8/A9 (Figure 2C) with (i) immobilized total RAGE; (ii) RAGE deglycosylated with PNGase F under non-denaturing conditions that removed both N-glycans and (iii) mAbGB3.1-enriched RAGE. Purified total RAGE binds S100A8/A9 with a K_d of ∼34.4 ± 13 nM and a Bmax (maximum binding sites) of 11.4 ± 2.2 mmol/mol RAGE [binding potential ($Bmax/K_d$) of 0.36 ± 0.07]. Deglycosylation almost completely abolished binding (Figure 2D). This shows that only a very small fraction (∼1%) of the RAGE molecules carry S100A8/A9-binding sites and that N-glycans contribute significantly to binding. In support of this, the subpopulation of RAGE enriched for carboxylated glycans by

mAbGB3.1 showed higher affinity interaction with a K_d of 7.62 ± 1.83 nM and a Bmax of 402.1 ± 30.5 mmol/mol RAGE (Figure 2D). This is a 35-fold increase in the molar binding and >100-fold increase in binding potential (Bmax/K_d of 55 ± 9.2), suggesting that carboxylated glycans form critical binding sites for S100A8/A9 on RAGE.

S100A8/A9 binds to colonic tumor cells in a carboxylated glycan-dependent manner promoting intracellular activation of NF-κB and cell proliferation

S100A8/A9 proteins are secreted in response to stimuli and have extracellular effects. To examine if S100A8/A9-binding sites are present on colon tumor cells, we performed a radioligand-binding assay using ^{125}I-labeled purified mouse S100A8/A9. CT-26 tumor cells showed specific saturable binding sites with a K_d of 35.09 ± 7.45 nM and a Bmax of 0.920 ± 0.077 pmol/million cells (Figure 3A). ^{125}I S100A8/A9 binding was displaced by 50-fold molar excess of cold ligand or 10-fold molar excess of anti-S100A8 (Figure 3B). To examine if the binding involves interaction with glycans on RAGE, we incubated cells with ^{125}I S100A8/A9 in the presence of mAbGB3.1 or anti-mouse RAGE. Binding was significantly reduced in the presence of mAbGB3.1 and anti-RAGE showing that RAGE and carboxylated glycans contribute to S100A8/A9 binding on tumor cells (Figure 3B).

Ligand binding to RAGE mediates downstream signaling events in cells leading to NF-κB activation. We therefore studied S100A8/A9-induced NF-κB activation in colon tumor cells using transient transfection with a luciferase expression plasmid containing four tandem repeats of NF-κB-binding site and *R.reniformis* luciferase expression construct as an internal control. The transfected cells were treated with endotoxin-free S100A8/A9. At low concentrations (0.5μg/ml, ∼20 nM), S100A8/A9 stimulated NF-κB-dependent transcription of luciferase within the cells. Preincubation with mAbGB3.1 or anti-RAGE prior to stimulation decreased NF-κB expression (Figure 3C), whereas an isotype control antibody had no or minimal effect (data not shown).

Since NF-κB activation plays an important role in intestinal cell survival and homeostasis (38), we next investigated whether S100A8/A9 promote colon tumor cell proliferation. Cells were untreated or treated with S100A8/A9 in low-serum medium in the presence or absence of inhibitors and cell proliferation was assayed using MTS reagent. At lower concentrations (1 μg/ml, ∼40 nM), S100A8/A9 induced significant cell growth (Figure 3D). Cell proliferation, however, did not increase with increasing concentrations of S100A8/A9 and only moderately with increasing time, similar to the effects of S100A8/A9 on human tumor cells (25). This suggests that S100A8/A9 may be rapidly internalized or degraded. mAbGB3.1 and anti-RAGE reduced S100A8/A9-induced early cellular proliferation (Figure 3D). Anti-RAGE also reduced cell proliferation in untreated cells, whereas mAbGB3.1 had no effect, suggesting that RAGE is important for tumor cell growth even in the absence of S100A8/A9, and S100A8/A9-induced cell proliferation may depend on carboxylated glycans expressed on RAGE and/or other proteins.

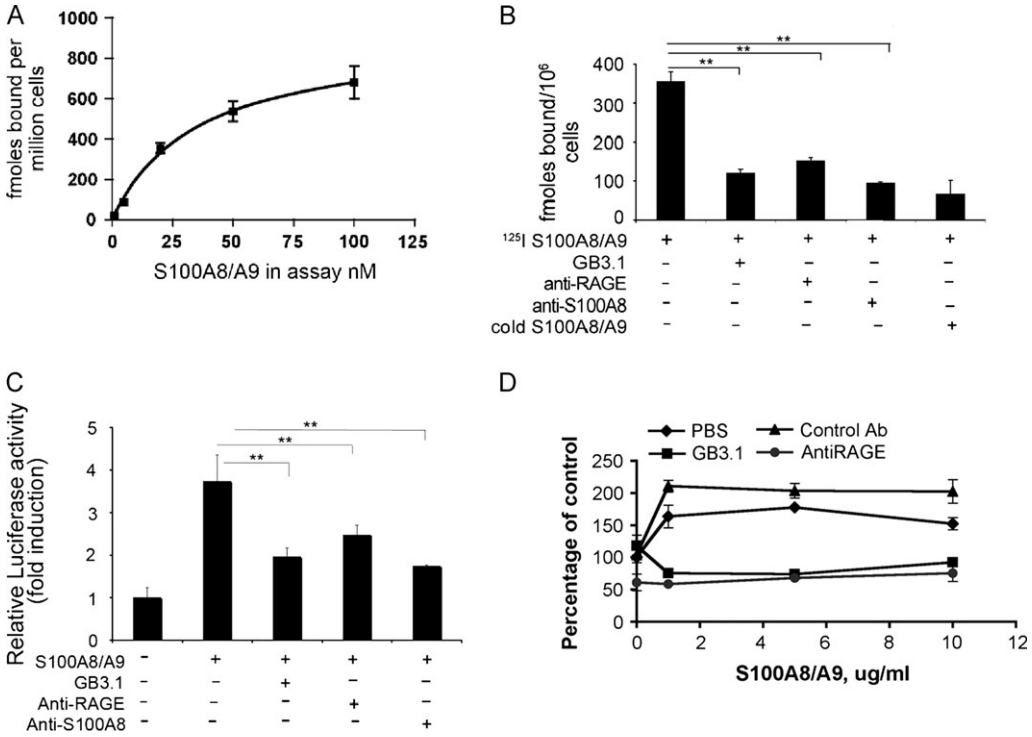

Fig. 3. (**A**) Binding of ^{125}I S100A8/A9 to CT-26 cells. Cells were incubated with increasing concentrations of ^{125}I S100A8/A9 for 1 h at 4°C followed by washing and cell lysis, and cell-bound radioactivity was measured using a gamma counter. Saturation binding kinetic analysis was performed using GraphPad Prism. Values represent mean ± SD of two determinations. (**B**) Inhibition of binding of ^{125}I S100A8/A9 to CT-26 cells. Cells were incubated with ^{125}I S100A8/A9 (20nM) in the presence or absence of mAbGB3.1, anti-RAGE or anti-S100A8 (10-fold molar excess) or cold ligand (50-fold molar excess). Cell-bound radioactivity was determined as above. Data represent mean ± SD of two determinations ($^{*}P \leq 0.05$ and $^{**}P \leq 0.01$). (**C**) S100A8/A9 induces NF-κB-dependent transcription. CT-26 cells were transiently transfected with plasmids containing firefly luciferase reporter gene under a promoter containing NF-κB-binding site and Renilla luciferase construct as an internal control. Transfected cells were stimulated with S100A8/A9 in presence or absence of inhibitors. Cell lysates were assayed for luciferase activity. Values are represented as ratio of firefly luciferase activity over Renilla luciferase (fold induction relative to unstimulated cells). Each value is the mean ± SD of two determinations ($^{*}P \leq 0.05$ and $^{**}P \leq 0.01$). (**D**) S100A8/A9 proteins stimulate colon cancer cell proliferation. CT-26 cells were incubated with increasing concentrations of S100A8/A9 in the presence or absence of mAbGB3.1, control antibody or anti-RAGE. At low concentrations, S100A8/A9 stimulated cell proliferation that was blocked by mAbGB3.1 and anti-RAGE. S100A8/A9-induced growth was not dependent on time or concentration as seen earlier with other tumor cells.

Myeloid progenitor cells expressing S100A8/A9 infiltrate colon tumors

To further understand the role of S100A8/A9, RAGE and carboxylated glycans in inflammation-induced tumorigenesis, we tested the effects of anti-carboxylated glycan antibody administration in a mouse model of CAC. Inflammation-induced colon carcinogenesis can be modeled in mice by injection of the procarcinogen AOM followed by a single or multiple exposures to DSS. DSS causes epithelial damage and activates macrophages inducing an acute colonic inflammation. This initial response progresses to chronic inflammation over time when adaptive immune system responses are triggered. Animals develop chronic inflammation, colonic dysplasia and adenoma within 12–20 weeks of combined administration of AOM and single or multiple cycles of DSS (4,39–41).

We induced CAC in mice using a single low dose of AOM followed by a single week of treatment with DSS (30,39). The animals exhibited weight loss and diarrhea during the acute phase that resolved within 1–2 weeks after DSS treatment. Six weeks after DSS, there were no clinical symptoms except for occasional soft stools. By 12–20 weeks, a few mice developed mild rectal prolapse and bloody stools. Histologically, there was significant colonic inflammation 2 weeks after DSS (Figure 4A, panel c, and Figure 5A). Colonic inflammation was appreciable at 6 weeks even though it was less severe than at 2 weeks (Figure 4A, panel d, and Figure 5A). In addition, low-grade dysplasia was evident at 6 weeks after initiation of disease, and by 12 weeks, all the mice developed high-grade dysplasias and adenomas (two to three tumors per mouse, 100% penetrance, Figure 4A, panels d–f). By 20 weeks, tumors were macroscopically visible (Figure 4A, panel g). Serum levels of NF-κB-dependent gene products TNFα and IL-6 were elevated 2 weeks after DSS and remained higher than normal 6 weeks after DSS (Figure 5B).

We observed diffuse staining for S100A8 and S100A9 in the colons 2 weeks after initiation (supplementary Figure 2 is available at *Carcinogenesis* Online). Expression of these proteins is restricted to neutrophils and immature macrophages or monocytes in early stage differentiation (42) and they are absent on mature macrophages (43). In addition, by 12–20 weeks of disease initiation, we found infiltrating cells positive for S100A8/A9 in all regions of dysplasia and adenoma (Figure 4B, panel a), similar to infiltration seen in human colon tumors (Figure 1), but they were absent in adjacent regions of no disease activity from the same colons (Figure 4B, panel b). The cells positive for S100A8/A9 were F4/80 negative, suggesting that they were not resident macrophages (data not shown).

To further understand the phenotypic nature of S100A8/A9-positive cells in tumors, we examined colons for $CD11b^+$ (monocyte), $Gr1^+$ (neutrophil) and $CD11b^+/Gr1^+$ (myeloid progenitor) cells. We found a few $CD11b^+$ cells in normal lamina propria, but $Gr1^+$ cells and double-positive cells were absent (data not shown). However, $CD11b^+$, $Gr1^+$ single-positive and $CD11b^+/Gr1^+$ double-positive cells were present in larger numbers in regions of dysplasia and tumors (Figure 4C). Immature myeloid progenitor cells are frequently found in tumors in mice and in many cancer patients (44–46). These cells identified phenotypically in mice as $Gr1^+CD11b^+$ cells and known as myeloid-derived suppressor cells (MDSCs) induce profound immune suppression against tumor antigens. MDSCs are also found in inflammation-induced skin tumors of wild-type mice but not in $RAGE^{-/-}$ tumors, suggesting that RAGE signaling may be required for recruitment MDSC (28). We found that MDSCs from mice

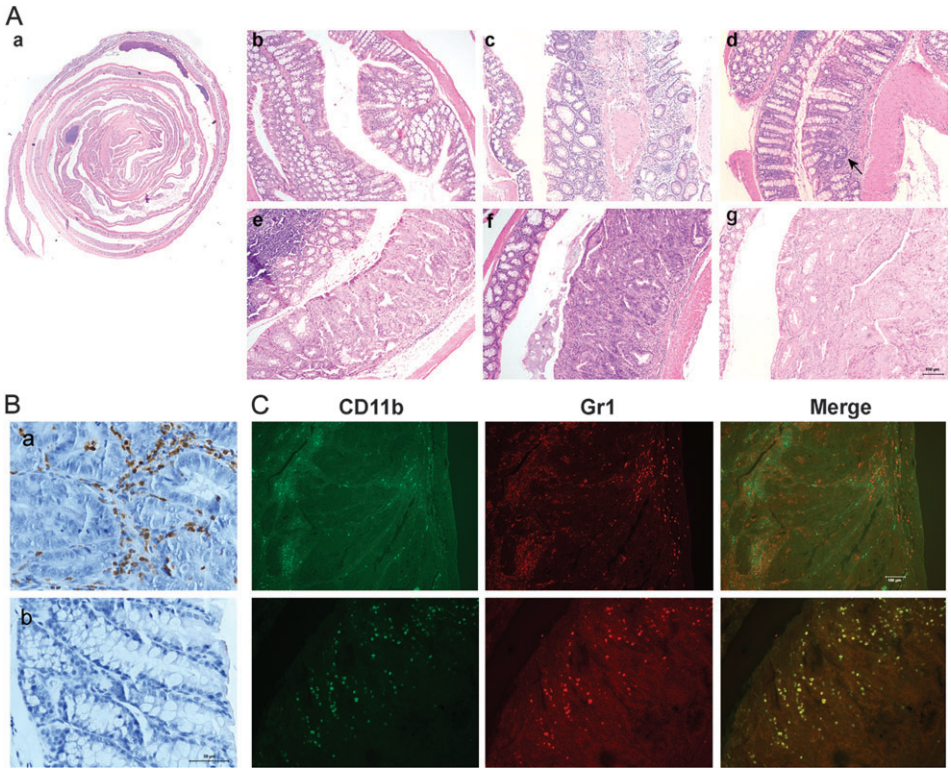

Fig. 4. (**A**) Representative hematoxylin and eosin-stained colon sections indicating progress of CAC in untreated wild-type mice subjected to the AOM–DSS protocol. (**a**) Normal colon Swiss-roll ×10 magnification. (**b**) Normal colon. (**c**) Colonic inflammation, 2 weeks after DSS. (**d**) Colonic inflammation, 6 weeks after DSS. Arrow indicates early dysplasia in a region of inflammation. (**e**) High-grade dysplasia (flat polypoid) 12 weeks after DSS. (**f**) Adenoma 12 weeks after DSS. (**g**) Adenoma 20 weeks after DSS. (**B**) (**a**) A representative tumor shows S100A9-positive infiltrating cells. Cells were also positive for S100A8 (data not shown). (**b**) A region adjacent to the tumor from the same colon is negative for S100A8/A9-positive cells. (**C**) Two representative sections of tumors with infiltrating cells stained for CD11b (myeloid) or Gr-1 (granulocyte). There was evidence for $CD11b^+$, $Gr\text{-}1^+$ single-positive and $CD11b^+/Gr\text{-}1^+$ double-positive cells within tumors representing infiltrating myeloid progenitors. Magnification scale bar is indicated for each panel.

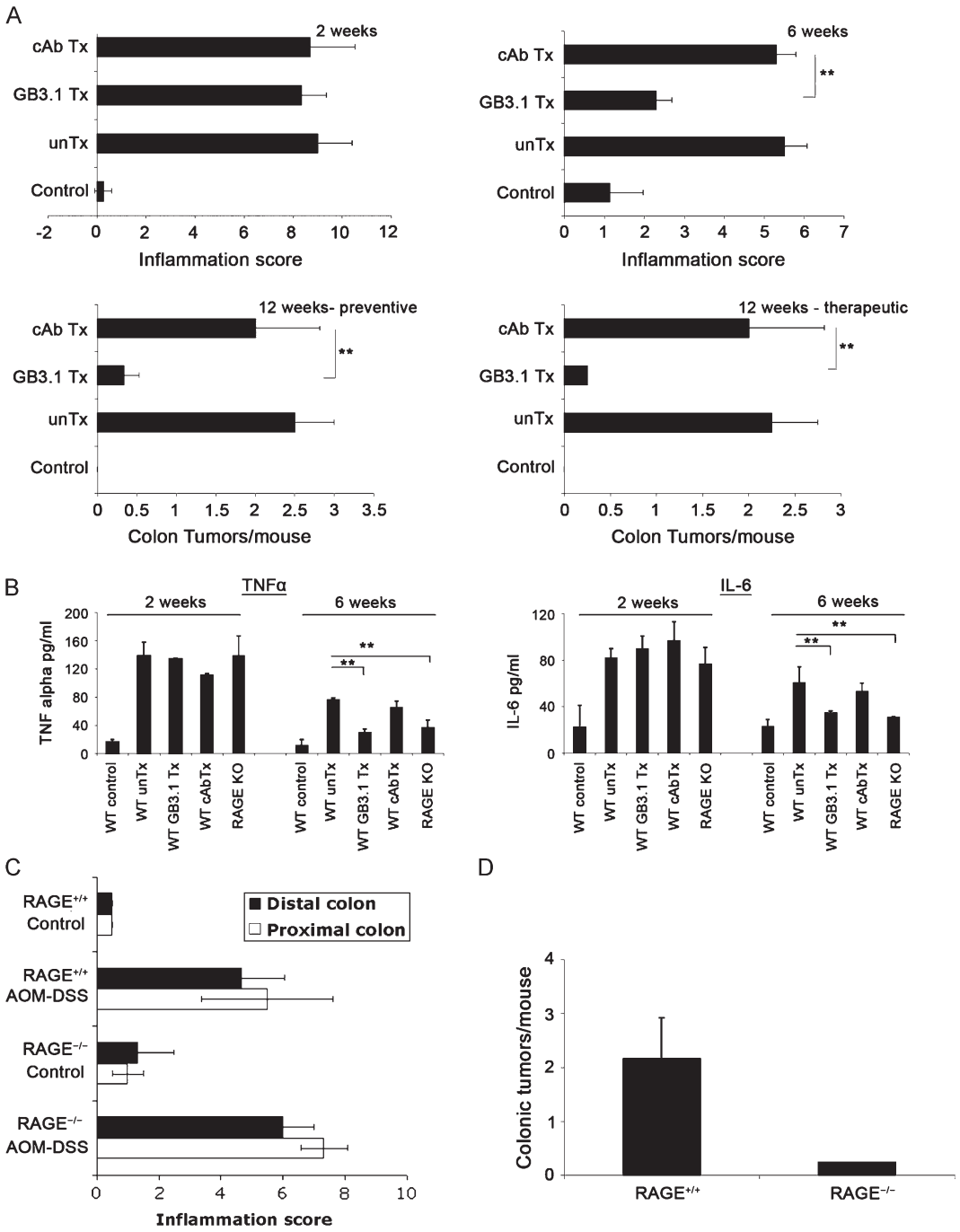

Fig. 5. (**A**) mAbGB3.1 administration reduces colonic inflammation (6 weeks) and incidence of tumors (12 weeks in preventive and therapeutic protocols) in mice treated with AOM–DSS. Mice were administered with mAbGB3.1 or a control antibody as described in Materials and Methods. Colonic inflammation, dysplasia and adenomas were evaluated using established criteria ($n = 4$ per group per time point, $^{**}P \leq 0.01$). (**B**) TNFα and IL-6 were measured in sera of mice at different time points ($n = 4$ per group per time point, $^{**}P \leq 0.01$). (**C**) Colonic inflammation in RAGE$^{+/+}$ and RAGE$^{-/-}$ mice 2 weeks after AOM–DSS evaluated using established criteria. (**D**) Colonic tumor incidence in RAGE$^{+/+}$ and RAGE$^{-/-}$ mice 20 weeks after AOM–DSS.

with mammary tumors show upregulation of intracellular S100A8/A9 and secrete them in response to stimuli (51). It is therefore probably that the S100A8/A9-positive cells in regions of colonic dysplasia and adenoma are immature myeloid progenitor cells adding to the heterogeneity of leukocyte populations within the tumor microenvironment.

Administration of anti-carboxylated glycan antibody reduces chronic inflammation and tumorigenesis

To investigate a functional role of the glycans in this model, we treated separate groups of AOM–DSS mice with mAbGB3.1 or isotype control antibody. mAbGB3.1 did not block the initial DSS-induced injury (2 weeks after DSS, Figure 5A), and treated mice did not show any difference in weight loss, clinical signs of inflammation or levels of proinflammatory cytokines in serum (Figure 5B), suggesting that the glycans may not play a role in the initial innate immune responses to DSS. However, administration of mAbGB3.1 reduced inflammation at 6 weeks and the incidence of tumors by ∼75% at 12 weeks after initiation (Figure 5A). In contrast, the control antibody-treated mice showed only a minimal decrease (20%) in incidence of inflammation and dysplasia. Levels of TNFα and IL-6 in

serum were also reduced in mAbGB3.1-treated mice at 6 and 12 weeks after initiation of disease (Figure 5B). These results suggest that reduction in tumor incidence in mAbGB3.1-treated mice is not due to block in initial acute colitis but due to block in transition to chronic inflammation and subsequent tumorigenesis. To establish whether the glycans independently promoted inflammation-mediated tumorigenesis, we examined the effect of antibody administration after establishment of chronic colitis. In fact, mAbGB3.1 treatment started 6 weeks after initiation of disease significantly reduced the incidence of dysplasia and adenoma (Figure 5A), suggesting that the glycans play dual roles in CAC, both in adaptive immune responses leading to chronic inflammation and in inflammation-mediated tumorigenesis.

RAGE-deficient mice are resistant to the onset of CAC

To evaluate the role of RAGE in S100A8/A9 and glycan-mediated signaling events leading to CAC, we applied the AOM–DSS protocol in RAGE$^{-/-}$ mice and wild-type mice. Both RAGE$^{-/-}$ and age-matched C57BL/6 wild-type mice lost up to 10% of body weight after DSS treatment before recovery (data not shown). Proximal and distal colons showed evidence of inflammation in both RAGE$^{-/-}$ mice and wild-type mice (Figure 5C) and serum TNFα and IL-6 levels were elevated in both groups (Figure 5B), demonstrating that RAGE does not play a role in the initial acute inflammatory events triggered by DSS. However, serum levels of the proinflammatory cytokines were reduced in the RAGE$^{-/-}$ mice at 6 weeks after disease initiation compared with wild-type mice (Figure 5B) and colonic inflammation was moderately reduced (supplementary Figure 3 is available at *Carcinogenesis* Online). In addition, there was a dramatic reduction in tumor incidence in RAGE$^{-/-}$ mice 20 weeks after AOM–DSS. Few dysplatic lesions found in RAGE$^{-/-}$ mice were small and low grade (data not shown). In contrast, all the wild-type mice developed adenomas (one to three tumors per mouse), with a few early invasive adenocarcinomas by 20 weeks. These findings show that RAGE is essential for the pathogenesis of CAC, complementing a recently published study on RAGE signaling in skin carcinogenesis (28) and highlighting the importance of RAGE in inflammation-mediated cancers.

Recent studies provide evidence for two different facets of inflammation-based cancers: persistent inflammation leading to cancer and a tumor-supporting role of inflammatory cells within the tumor microenvironment in the absence of inflammation. Both facets reflect the functional plasticity of macrophages (47). RAGE expressed on macrophages, endothelial cells and tumor cells and S100A8/A9 expressed on infiltrating leukocytes are implicated both in inflammation and cancer. Here, we provide direct evidence that carboxylated glycans expressed on a subpopulation of RAGE on tumor cells provide critical binding sites for S100A8/A9. The glycans and RAGE also mediate S100A8/A9-induced downstream signaling in tumor cells and cell proliferation. Using a colitis-induced cancer model that involves an acute inflammation phase, a chronic inflammation phase and a tumorigenesis phase, we also show that the glycans and RAGE are important both in the chronic inflammation and tumorigenesis phases. S100A8/A9-positive cells are found both in inflamed tissues and within tumor stroma. These findings, along with our earlier studies on T cell-mediated colitis, suggest that the glycans, RAGE and S100A8/A9 are important in both facets of inflammation-based cancers. However, *in vivo*, the importance of other RAGE ligands such as HMGB1, which bind carboxylated glycans, cannot be ruled out since HMGB1 induces IL-6 in macrophages via NF-κB activation, and administration of anti-HMGB1 decreases CAC in Apc/Min^{+} mice (48).

The signals and stage of disease that trigger the expression of carboxylated glycans and RAGE on colon tumor cells and of the stimuli that promote infiltration of S100A8/A9-positive myeloid progenitors within the tumors are not known. Mediators such as vascular endothelial growth factor, TNFα and transforming growth factor-β secreted in response to inflammation or tumor hypoxia mobilize S100A8/A9-positive cells that promotes premetastatic niches in lung facilitating homing of tumor cells to metastatic sites (49). We also found that S100A8/A9 could serve as autocrine mediators that sustain a feedback loop and accumulation of MDSCs within tumors (51). S100A8/A9 is also expressed by infiltrating macrophages in early acute colitis (supplementary Figure 2 is available at *Carcinogenesis* Online). Since S100A8/A9 also bind Toll-like receptor 4 (TLR4) (20), S100A8/A9 secreted from activated leukocytes could play a role in amplifying initial DSS-mediated responses induced by bacterial lipopolysaccharide through interaction with TLR4 on macrophages. This T cell-independent initial innate response may not involve RAGE or the glycans since mAbGB3.1 does not block it, and RAGE$^{-/-}$ mice are as susceptible to DSS-induced injury as RAGE$^{+/+}$ mice (Figure 5). The importance of TLR4 in the development of CAC is evident from the finding that TLR4-deficient mice are protected from CAC (50). S100A8/A9 could therefore participate in distinct events in disease progression through different receptors: an acute inflammation phase involving TLR4 and a tumorigenesis and progression phase involving the glycans and RAGE expressed on tumor cells.

In summary, our findings show that RAGE, S100A8/A9 and carboxylated glycans form important components of epithelial and stromal cells promoting molecular interactions leading to CAC. This complex signaling pathway could be a potential target for pharmacological interventions.

Supplementary material

Supplementary Figures 1–3 can be found at http://carcin.oxfordjournals.org/

Funding

National Institutes of Health (R01-CA92608) to H.H.F. and G.S.; Broad Medical Research Program of the Eli and Edythe L. Broad Foundation and Crohn's and Colitis Foundation of America (to H.H.F., G.S. and M.K.); Dr Howard and Barbara Milstein Endowment fund and gift from Howard and Carole Goldfeder (to H.H.F.); Deutsche Forschungsgemeinschaft (DFG/SFB 405) to P.P.N. and A.B.; Research Corporation Technologies, Tucson, AZ, funded the human tissue work.

Acknowledgements

We thank Dr Achim Temme and Dr Bernd Weigle of the Institute of Immunology, Technical University, Dresden, Germany, for their kind gift of sRAGE expressing HeLa cells; Adriana Charbono and Buddy Charbono for their invaluable help with the animal experiments; the vivarium staff for excellent care of the RAGE$^{-/-}$ colony; Gia Garcia, Ronald Torres and Lisa Wiggleton for help with histology; Dr Chui Sien Chan for the genotyping protocol for RAGE$^{-/-}$ mice and Douglas Haynes and Harish Khandrika for help with illustrations. We also thank Dr Takuji Tanaka, Kanazawa Medical University, Ishikawa, Japan, for valuable advice on the AOM-DSS model and Dr Suzanne Ostrand-Rosenberg, University of Maryland, Baltimore, for critical reading of the manuscript.

Conflict of Interest Statement: None declared.

References

1. Itzkowitz,S.H. *et al*. (2004) Inflammation and cancer IV. Colorectal cancer in inflammatory bowel disease: the role of inflammation. *Am. J. Physiol. Gastrointest. Liver Physiol.*, **287**, G7–G17.
2. Mantovani,A. (2005) Cancer: inflammation by remote control. *Nature*, **435**, 752–753.
3. Condeelis,J. *et al*. (2006) Macrophages: obligate partners for tumor cell migration, invasion, and metastasis. *Cell*, **124**, 263–266.
4. Greten,F.R. *et al*. (2004) IKKbeta links inflammation and tumorigenesis in a mouse model of colitis-associated cancer. *Cell*, **118**, 285–296.
5. Karin,M. *et al*. (2005) NF-kappaB: linking inflammation and immunity to cancer development and progression. *Nat. Rev. Immunol.*, **5**, 749–759.

6. Schmidt,A.M. *et al*. (2001) The multiligand receptor RAGE as a progression factor amplifying immune and inflammatory responses. *J. Clin. Invest.*, **108**, 949–955.
7. Bierhaus,A. *et al*. (2005) Understanding RAGE, the receptor for advanced glycation end products. *J. Mol. Med.*, **83**, 876–886.
8. Bierhaus,A. *et al*. (2006) RAGE in inflammation: a new therapeutic target? *Curr. Opin. Investig. Drugs*, **7**, 985–991.
9. Li,J. *et al*. (1997) Characterization and functional analysis of the promoter of RAGE, the receptor for advanced glycation end products. *J. Biol. Chem.*, **272**, 16498–16506.
10. Bierhaus,A. *et al*. (2001) Diabetes-associated sustained activation of the transcription factor nuclear factor-kappaB. *Diabetes*, **50**, 2792–2808.
11. Srikrishna,G. *et al*. (2001) A novel anionic modification of N-glycans on mammalian endothelial cells is recognized by activated neutrophils and modulates acute inflammatory responses. *J. Immunol.*, **166**, 624–632.
12. Norgard-Sumnicht,K.E. *et al*. (1995) Unusual anionic N-linked oligosaccharides from bovine lung. *J. Biol. Chem.*, **270**, 27634–27645.
13. Srikrishna,G. *et al*. (2005) Novel carboxylated N-glycans contain oligosaccharide-linked glutamic acid. *Biochem. Biophys. Res. Commun.*, **332**, 1020–1027.
14. Srikrishna,G. *et al*. (2002) N-glycans on the receptor for advanced glycation end products influence amphoterin binding and neurite outgrowth. *J. Neurochem.*, **80**, 998–1008.
15. Srikrishna,G. *et al*. (2001) Two proteins modulating transendothelial migration of leukocytes recognize novel carboxylated glycans on endothelial cells. *J. Immunol.*, **166**, 4678–4688.
16. Srikrishna,G. *et al*. (2005) Carboxylated glycans mediate colitis through activation of NF-{kappa}B. *J. Immunol.*, **175**, 5412–5422.
17. Foell,D. *et al*. (2007) S100 proteins expressed in phagocytes: a novel group of damage-associated molecular pattern molecules. *J. Leukoc. Biol.*, **81**, 28–37.
18. Hermani,A. *et al*. (2006) S100A8 and S100A9 activate MAP kinase and NF-kappaB signaling pathways and trigger translocation of RAGE in human prostate cancer cells. *Exp. Cell Res.*, **312**, 184–197.
19. Sunahori,K. *et al*. (2006) The S100A8/A9 heterodimer amplifies proinflammatory cytokine production by macrophages via activation of nuclear factor kappa B and p38 mitogen-activated protein kinase in rheumatoid arthritis. *Arthritis Res. Ther.*, **8**, R69.
20. Vogl,T. *et al*. (2007) Mrp8 and Mrp14 are endogenous activators of Toll-like receptor 4, promoting lethal, endotoxin-induced shock. *Nat. Med.*, **13**, 1042–1049.
21. Gebhardt,C. *et al*. (2006) S100A8 and S100A9 in inflammation and cancer. *Biochem. Pharmacol.*, **72**, 1622–1631.
22. Donato,R. (2001) S100: a multigenic family of calcium-modulated proteins of the EF-hand type with intracellular and extracellular functional roles. *Int. J. Biochem. Cell Biol.*, **33**, 637–668.
23. Roth,J. *et al*. (2003) Phagocyte-specific S100 proteins: a novel group of proinflammatory molecules. *Trends Immunol.*, **24**, 155–158.
24. Hermani,A. *et al*. (2005) Calcium-binding proteins S100A8 and S100A9 as novel diagnostic markers in human prostate cancer. *Clin. Cancer Res.*, **11**, 5146–5152.
25. Ghavami,S. *et al*. (2008) S100A8/A9 at low concentration promotes tumor cell growth via RAGE ligation and MAP kinase-dependent pathway. *J. Leukoc. Biol.*, **83**, 1484–1492.
26. Ehlermann,P. *et al*. (2006) Increased proinflammatory endothelial response to S100A8/A9 after preactivation through advanced glycation end products. *Cardiovasc. Diabetol.*, **5**, 6.
27. Boyd,J.H. *et al*. (2008) S100A8 and S100A9 mediate endotoxin-induced cardiomyocyte dysfunction via the receptor for advanced glycation end products. *Circ. Res.*, **102**, 1239–1246.
28. Gebhardt,C. *et al*. (2008) RAGE signaling sustains inflammation and promotes tumor development. *J. Exp. Med.*, **205**, 275–285.
29. Liliensiek,B. *et al*. (2004) Receptor for advanced glycation end products (RAGE) regulates sepsis but not the adaptive immune response. *J. Clin. Invest.*, **113**, 1641–1650.
30. Suzuki,R. *et al*. (2004) Sequential observations on the occurrence of preneoplastic and neoplastic lesions in mouse colon treated with azoxymethane and dextran sodium sulfate. *Cancer Sci.*, **95**, 721–727.
31. Hunter,M.J. *et al*. (1998) High level expression and dimer characterization of the S100 EF-hand proteins, migration inhibitory factor-related proteins 8 and 14. *J. Biol. Chem.*, **273**, 12427–12435.
32. Harada,O. *et al*. (2007) The role of trophinin, an adhesion molecule unique to human trophoblasts, in progression of colorectal cancer. *Int. J. Cancer*, **121**, 1072–1078.
33. Stulik,J. *et al*. (1999) The analysis of S100A9 and S100A8 expression in matched sets of macroscopically normal colon mucosa and colorectal carcinoma: the S100A9 and S100A8 positive cells underlie and invade tumor mass. *Electrophoresis*, **20**, 1047–1054.
34. Sickert,D. *et al*. (2007) Characterization of macrophage subpopulations and microvessel density in carcinomas of the gastrointestinal tract. *Anticancer Res.*, **27**, 1693–1700.
35. Hofmann,M.A. *et al*. (1999) RAGE mediates a novel proinflammatory axis: a central cell surface receptor for S100/calgranulin polypeptides. *Cell*, **97**, 889–901.
36. Huttunen,H.J. *et al*. (2000) Coregulation of neurite outgrowth and cell survival by amphoterin and S100 proteins through receptor for advanced glycation end products (RAGE) activation. *J. Biol. Chem.*, **275**, 40096–40105.
37. Fuentes,M.K. *et al*. (2007) RAGE activation by S100P in colon cancer stimulates growth, migration, and cell signaling pathways. *Dis. Colon Rectum*, **50**, 1230–1240.
38. Jobin,C. *et al*. (2000) The I kappa B/NF-kappa B system: a key determinant of mucosalinflammation and protection. *Am. J. Physiol. Cell Physiol.*, **278**, C451–C462.
39. Tanaka,T. *et al*. (2003) A novel inflammation-related mouse colon carcinogenesis model induced by azoxymethane and dextran sodium sulfate. *Cancer Sci.*, **94**, 965–973.
40. Dieleman,L.A. *et al*. (1998) Chronic experimental colitis induced by dextran sulphate sodium (DSS) is characterized by Th1 and Th2 cytokines. *Clin. Exp. Immunol.*, **114**, 385–391.
41. Melgar,S. *et al*. (2005) Acute colitis induced by dextran sulphate sodium progresses into chronicity in C57BL/6 but not in BALB/c mice—correlation between symptoms and inflammation. *Am. J. Physiol. Gastrointest. Liver Physiol.*, **288**, G1328–1338.
42. Roth,J. *et al*. (1993) Expression of calcium-binding proteins MRP8 and MRP14 is associated with distinct monocytic differentiation pathways in HL-60 cells. *Biochem. Biophys. Res. Commun.*, **191**, 565–570.
43. Odink,K. *et al*. (1987) Two calcium-binding proteins in infiltrate macrophages of rheumatoid arthritis. *Nature*, **330**, 80–82.
44. Sinha,P. *et al*. (2005) Tumor immunity: a balancing act between T cell activation, macrophage activation and tumor-induced immune suppression. *Cancer Immunol. Immunother.*, **54**, 1137–1142.
45. Serafini,P. *et al*. (2006) Myeloid suppressor cells in cancer: recruitment, phenotype, properties, and mechanisms of immune suppression. *Semin. Cancer Biol.*, **16**, 53–65.
46. Nagaraj,S. *et al*. (2007) Myeloid-derived suppressor cells. *Adv. Exp. Med. Biol.*, **601**, 213–223.
47. Sica,A. *et al*. (2008) Cancer related inflammation: the macrophage connection. *Cancer Lett.*, **267**, 204–215.
48. Maeda,S. *et al*. (2007) Essential roles of high-mobility group box 1 in the development of murine colitis and colitis-associated cancer. *Biochem. Biophys. Res. Commun.*, **360**, 394–400.
49. Hiratsuka,S. *et al*. (2006) Tumour-mediated upregulation of chemoattractants and recruitment of myeloid cells predetermines lung metastasis. *Nat. Cell Biol.*, **8**, 1369–1375.
50. Fukata,M. *et al*. (2007) Toll-like receptor-4 promotes the development of colitis-associated colorectal tumors. *Gastroenterology*, **133**, 1869–1881.
51. Sinha,P. *et al*. (2008) Proinflammatory S100 proteins regulate the accumulation of myeloid derived suppressor cells. *J. Immunol*., in press.

Received May 16, 2008; revised July 25, 2008; accepted August 3, 2008